1 **[Title Page]**

2 **Unburned carbon measurement in fly ash using laser-induced breakdown spectroscopy with short**

3 **nanosecond pulse width laser**

4

5 Renwei Liu[a,b], Yoshihiro Deguchi[b,c]*, Weigang Nan[b,d], Ruomu Hu[a], Zhenzhen Wang[b,c], Yuki Fujita[b], Seiya

6 Tanaka[b], Kazuki Tainaka[e], Kenji Tanno[e], Hiroaki Watanabe[f], Jiping Liu[a], and Junjie Yan[c]

7

8 [a] Moe Key Laboratory of Thermo-Fluid Science and Engineering, Xi'an Jiaotong University, Xi'an, 710049,

9 China.

10 [b] Graduate School of Advanced Technology and Science, Tokushima University, Tokushima, 770-8501,

11 Japan.

12 [c] State Key Laboratory of Multiphase Flow in Power Engineering, Xi'an Jiaotong University, Xi'an, 710049,

13 China.

14 [d] School of Energy and Power Engineering, Xi'an Jiaotong University, Xi'an, 710049, China.

15 [e] Energy Engineering Research Laboratory, The Central Research Institute of Electric Power Industry,

16 Kanagawa, 240-0196, Japan.

17 [f] Department of Mechanical Engineering, Kyushu University, Fukuoka, 819-0395, Japan.

18

19 Corresponding author: Yoshihiro Deguchi

20 Graduate School of Advanced Technology and Science, Tokushima University

21 TEL: (+81)-88-656-7375

22 FAX: (+81)-88-656-9082

23 Email address: ydeguchi@tokushima-u.ac.jp

24 Postal address: 2-1, Minamijyosanjima, Tokushima 770-8506 Japan

25

26   **[Abstract]**

27   **Unburned carbon measurement in fly ash using laser-induced breakdown spectroscopy with short**

28   **nanosecond pulse width laser**

29

30   Renwei Liu, Yoshihiro Deguchi, Weigang Nan, Ruomu Hu, Zhenzhen Wang, Yuki Fujita, Seiya Tanaka,

31   Kazuki Tainaka, Kenji Tanno, Hiroaki Watanabe, Jiping Liu, and Junjie Yan

32

33   **Abstract**

34   The unburned carbon in fly ash is one of the important factors for the boiler combustion condition.

35   Controlling the unburned carbon in fly ash is beneficial for fly ash recycle and to improve the combustion

36   efficiency of the coal. Laser-induced breakdown spectroscopy (LIBS) technology has been applied to

37   measure the fly ash contents due to its merits of non-contact, fast response, high sensitivity, and real-time

38   measurement. In this study, experimental measurements have been adopted for fly ash flows with the

39   surrounding gases of N_2 and CO_2, while the CO_2 concentration varified to evaluate the CO_2 effect on the

40   unburned carbon signal from fly ash powder. Two kinds of pulse width lasers, 6ns and 1ns, were separately

41   adopted to compare the influence of laser pulse width. Results showed that compared with 6ns pulse width

42   laser, plasma temperature was lower and had less dependence on delay time when using 1ns pulse width

43   laser, and spectra had more stable background. By using 1ns pulse width laser, the emission signal from

44   surrounding CO_2 also decreased because of the less surrounding gas breakdown. The solid powder

45   breakdown signals also became more stable when using 1ns pulse width laser. So it is demonstrated that 1ns

46   pulse width laser has the merits for fly ash flow measurement using LIBS.

47

48   **Keywords:** laser-induced breakdown spectroscopy; fly ash powder flow; short nanosecond pulse width

49   laser; solid powder breakdown; surrounding gas breakdown.

50

1. Introduction

The unburned carbon in fly ash is one of the important factors to evaluate the combustion efficiency of the boiler [1-3]. A fast-response measurement method of unburned carbon in fly ash can improve the control of boiler combustion. The improvement of the boiler combustion efficiency is beneficial for the fuels saving and the environment protection. Recycling the fly ash as the source of concrete is also important for its useful utilization. The carbon content in the fly ash is not conducive to its recycling. Therefore, the carbon content should be controlled. The online measurement of fly ash compositions is helpful to control the carbon content in time, because of the continuous coal combustion. The variation range of the unburned carbon in fly ash is very different for different boilers and combustion conditions. For large capacity boilers, the ash carbon content is usually about 2-15% [4]. For circulating fluidized bed boilers, it is about 10-20% [5]. When the coals species and load change in the plant, the fly ash content is also different.

A variety of fly ash detection methods have been proposed and applied in fly ash measurement. The traditional methods, such as thermal gravimetric analysis method, microwave attenuation method, and electrostatic capacitance measurement method and so on [6, 7], are widely applied. X-ray diffraction (XRD) powder analysis or SEM methods [1, 8-11] have also been applied to measure the compositions and microstructure of the fly ash. For online measurement, however, these methods meet the difficulties due to the sample preparation. Therefore, laser-induced breakdown spectroscopy (LIBS) is proposed for fly ash measurement due to its merits of non-contact, fast-response, multi-element detection and online measurement. Up to now, LIBS technology has been applied in different fields such as power plants, steel making processes, environment, marine, food safety, and so on [12-14].

LIBS measurements of fly ash have also attracted much attention. The measurement properties and quantitative analysis method of fly ash were extensively studied [3, 15-23]. The influence of ambient pressure and temperature, powder sizes, laser energy and so on were discussed [3, 15-17]. Some calibration methods were proposed [18-21] to improve the quantitative measurement, such as internal standard method, plasma temperature correction method, multivariate calibration method, wavelet neural method. In some studies [22, 23], the fly ash samples were prepared as pellet to detect the elements of Ca, Mg, Fe and so on.

3

78　For the online measurement of fly ash flow in the boiler, LIBS measurement of fly ash has its own problem.

79　LIBS measurement of powder flow should consider both the solid powder breakdown and the surrounding

80　gas breakdown. Besides, the components of flue gas are very complex, such as NO_X, SO_X, CO_2 and so on.

81　The concentration of CO_2 is usually up to the level of around 10% [24]. The induced CO_2 plasma emits the

82　carbon signal which introduces measurement error to the unburned carbon content of fly ash powder [25].

83　To reduce the CO_2 effect, the measurement systems were designed and applied to reduce CO_2 concentration

84　[26-28], which were able to measure the fly ash flow continuously. For example, a cyclone system was

85　applied to separate the fly ash powder with the flue gas [26]. Another system was designed as that the fly ash

86　was dropped onto the conveying belt. The measurement position was covered by a chamber when

87　introducing air to reduce the CO_2 concentration [27, 28]. Reduction of CO_2 concentration by sampling and

88　measurement systems was a valid method to reduce the CO_2 influence on unburned carbon signal for online

89　measurement of fly ash. However, the detailed influence of CO_2 on unburned carbon signal was not

90　discussed entirely in these studies. Because the CO_2 effect is rather sensitive to the concentration in

91　surrounding gas and less than 1% CO_2 causes the spurious C signal in LIBS spectra of fly ash [26].

92　　The control of the solid powder breakdown and surrounding gas breakdown is also a way to decrease the

93　surrounding gas effects. The laser pulse width is one important factor for laser-induced plasma, and many

94　researches have testified the pulse width effects on LIBS measurement [29-35] for both gas-phase target and

95　solid measurement. For gas-phase target measurement, the shorter pulse width laser induced a better target

96　element measurement. For solid measurement, when using the shorter pulse width laser, more laser beam

97　energy was concentrated on the solid surface, and craters on solid surface became more regular, such as

98　picosecond or femtosecond laser. So the LIBS detection ability can be improved, such as the higher signal to

99　noise ratio, lower background emission. Therefore, the laser-induced plasma processes of solid powder and

100　surrounding gas can be changed when using different pulse width lasers. In this study, the CO_2 effect on the

101　unburned carbon signal was studied according to the laser-induced plasma processes. Two different

102　nanosecond pulse width lasers were employed to discuss the laser-induced plasma processes of fly ash flow.

103

104　**2. Theory**

105

106   In the LIBS measurement of powder flow, the sample is in the multi-phase condition including solid

107   powder and surrounding gas. The laser-induced plasma formation processes of the solid powder and its

108   surrounding gas can be summarized as follow [35, 36]: When the laser beam is focused on the sample, the

109   solid powders firstly absorb energy and evaporate as the material vapour. Plasma is firstly generated within

110   the material vapour. Because of the high pressure and temperature, the material vapour and plasma expand

111   and mix with the surrounding gas and the residual part of the powder, which are also broken down through

112   the electron collision, which can be enhanced through plasma reheating by laser pulse. The formation and

113   development processes of plasma are illustrated in Fig.1. Fig.1 (a) is the plasma structure concept of the

114   solid powder with the surrounding gas. When the laser energy is small, surrounding gas cannot be broken

115   down directly due to its high breakdown threshold [19]. So the solid powder plasma is firstly generated, then

116   expands and induces the breakdown of surrounding gas. Fig.1 (b) shows the diagram of different laser pulse

117   width, and Fig.1 (c) illustrates the concept of differences of plasma evolution processes using different pulse

118   width lasers. As mentioned in plasma formation processes, there is a time gap between the beginning time of

119   solid breakdown and gas breakdown, while the end time of breakdown is near to the end time of laser pulse.

120   When the laser pulse width becomes shorter, the time of plasma reheating by laser pulse will be shorter [30],

121   and more plasma is formed within the solid material vapour. What's more, when the laser pulse energy is

122   same, the peak power is higher when the pulse width is shorter, as shown in Fig.1 (b), and more laser pulse

123   energy is allocated to solid breakdown. In this way, the solid powder breakdown and surrounding gas

124   breakdown can be controlled by the laser pulse width. Previously, the pulse width influence was discussed

125   by comparing the nanosecond laser with picosecond or femtosecond lasers. The shorter pulse width laser can

126   better concentrate energy for the target breakdown, but the complex laser system challenges their on-line

127   applications. It has been mentioned [36] that the time of solid evaporation is usually within 1ns; while up to

128   around 5ns, the material vapour expands to induce the surrounding gas breakdown. Therefore, even if 1ns

129   pulse width, the plasma formation processes may also have obvious difference. Besides, 1ns nanosecond

130   laser can keep its relative structure simplicity, which is good for online measurement.

131   The analysis of LIBS is usually based on the signal intensity of characteristic lines. The theoretical

132   equation between the signal intensity and the concentration of measured species with the local thermal

133   equilibrium (LTE) assumption has been proposed. The detailed explanation is shown in elsewhere [12]. The

134   signal can be calculated as the ratio of $I_{target}/I_{reference}$ [16, 20, 27] to discard the absolute intensity fluctuation

135   influence of the spectra. Plasma temperature is one of the main influencing factors for signal variation. To

136   evaluate plasma temperature, similar as the Saha-Boltzmann multi-line graph theory [37], the plasma

137   temperature indicator is proposed [3]. Plasma temperature indicator is defined as the ratio of same element

138   from different upper energy levels: $I_{i,j1}/I_{i,j2}$. i means the emission element, j1, j2 mean different upper energy

139   levels. According to the relation between $I_{target}/I_{reference}$ and $I_{i,j1}/I_{i,j2}$, the plasma temperature correction factor

140   can be determined [5, 19, 26]. Plasma temperature correction method is applied to reduce the influence of

141   plasma temperature fluctuation on the signal intensity. In this study, I_{Mg1}/I_{Mg2} was defined as the plasma

142   temperature indicator. The functional relation between I_C/I_{Si1} and I_{Mg1}/I_{Mg2} was fitted into some exponential

143   relation and the exponential term of I_{Mg1}/I_{Mg2} was the temperature correction factor, which can be calculated

144   theoretically but actually determined according to the experiment due to the complex laser-induced plasma

145   processes [3, 16].

146

147   **3. Experimental**

148

149   The experimental diagram of fly ash measurement using LIBS is presented in Fig.2. It contained two

150   lasers, a spectrometer, an ICCD camera and auxiliary equipment. These two lasers were both nanosecond

151   lasers with different pulse widths operating at 1064nm. The laser marked as Laser 1 was a laser with the

152   pulse width of 6ns (LOTIS TII 2132-UTF). The laser marked as Laser 2 was a laser with the pulse width of

153   1ns (Hamamatsu Photonics, Microchip Laser L12968-01). During the experiment, one laser was operated

154   and the optical path of laser beam was altered by the up-and-down adjustment of Mirror 2. Both lasers were

155   operated at the frequency of 10Hz. The Focus Lens 1 with the focal length of 200mm was employed to focus

156   the laser beams onto the fly ash powder flow. In order to compare the influence of laser pulse width on fly

157   ash measurement, the conditions of these two laser beams including laser energy, beam shape, beam

158   diameter and beam axis in front of Focus Lens 1 at the same point were adjusted to the same by a series of

159   optical components. The laser energy was 7mJ/pulse and the beam diameter was 8mm. The low laser energy

160   was set to induce solid powder plasma and to avoid the direct breakdown of surrounding gas. Because of the

161   transmittance of the gas, its breakdown threshold is usually higher than that of solid [29, 38, 39]. In this

162   study it was testified that 7mJ/pulse is lower than the gas breakdown threshold and it cannot induce the gas

163   breakdown directly. The plasma emission was detected at the coaxial direction with the laser beam. The

164   plasma emission was reflected by a filter that reflects the light below 400nm, and then focused onto the fiber

165   by the Focus Lens 2 with the focal length of 220mm.

166   The emission signals from the plasma were detected by the combination of a spectrometer (SOL, NP-250-

167   2), an ICCD camera (Andor, iStar DH334T-18U-03), and auxiliary equipment. The spectrometer with two

168   channels was employed, which can simultaneously detect the spectra with different resolution when using

169   the different gratings. In this study, the resolution of Channel 1 was 0.076nm/pixel with the grating of

170   600l/mm. The wavelength region was 240~320nm. The resolution of Channel 2 was 0.012nm/pixel with the

171   grating of 3600l/mm. The wavelength region was 244~256nm. The gate width was set as 500ns. The delay

172   time was different when using different pulse width lasers. When Laser 1 was used, the delay time was 300,

173   500, 800, 1000, 1500ns. When Laser 2 was used, the delay time was 5, 10, 25, 50, 100ns. The accumulation

174   was 100 times of laser shot and the experimental result under the same condition was measured 3 times.

175   In this study, the employed fly ash sample with unburned carbon of 24.9% was sampled from a furnace in

176   the lab. The compositions of fly ash were checked by the conventional chemical analysis methods (Japanese

177   Industrial Standards JIS-M-8801, JIS-M-8815) [16]. The main components of fly ash sample are listed in

178   Table 1. The fly ash was introduced to the measurement area by a feeder (Nisshin Engineering Inc. Feedcon-

179   μ Mtype). The feeding speed of the feeder was 200mg/min. A chamber covered the exit of the feeder to mix

180   the fly ash with the surrounding gas of N_2 and CO_2 mixture. The N_2 and CO_2 were pre-mixed before

181   introducing into the chamber. The pre-mixed surrounding gas was divided into two flows to totally cover

182   and mix the fly ash powder under the N_2 and CO_2 mixture condition during the measurement process. One

183   surrounding gas flow was introduced from the top of the chamber with the flow rate of 1L/min. The fly ash

184   dropped out from the outlet pipe with the diameter of 3mm. Another gas was introduced to the underside of

185 the chamber to surround the outlet of pipe, with the flow rate of 4L/min. In order to clarify the CO_2 effect in

186 this study, the CO_2 volume percentage was set as 0%, 1.30%, 3.80%, and 6.18% in the measurement system.

187 The laser beam was focused closely to this outlet pipe to ensure the measured fly ash mixed with the

188 surrounding gas of N_2 and CO_2 mixture.

189

190 **4. Results and Discussion**

191

192   The spectrometer employed in this study with two channels can measure two wavelength ranges of the

193 spectra simultaneously. The main elements in fly ash, such as C, Si, Al, Fe, Ca, Mg, were measured using

194 Channel 1 with the wide wavelength range from 240nm to 320nm, with the resolution of 0.076nm/pixel.

195 According to the previous studies, the C emission line at 247.86nm can be interfered by the neighbor lines

196 such as Fe line at 247.98nm [11, 40, 41]. In order to clarify the unburned carbon in fly ash, the clear C

197 emission line was detected using Channel 2 with the wavelength range from 244nm to 256nm, with the

198 resolution of 0.012nm/pixel. The C content of fly ash sample employed in this study was 24.9% to discuss

199 the surrounding gas effect on the solid powder measurement. It was verified that Fe line showed less

200 interference on C signal in this study.

201   The typical measured spectra of fly ash without CO_2 using Laser 1 with the pulse width of 6ns is shown in

202 Fig.3. The measured species and their specific wavelengths are listed in Table 2 according to the NIST

203 database [42]. The emission intensity of the spectra in this paper was normalized with the corresponding

204 maximum signal in each measured result.

205     $I_{target}/I_{reference}$ and $I_{i,j1}/I_{i,j2}$ were defined according to the ratios of the characteristic emission lines, which

206 were selected from the same channel. For the $I_{target}/I_{reference}$, Si was selected as the reference element, because

207 Si was a major component in fly ash. For unburned carbon measurement, the ratio of C (247.86nm)/Si1

208 (251.61nm) in Channel 2 was used to evaluate the carbon content [3, 16]. Other elemental signals should

209 also be considered [3], such as the ratio of Fe/Si2, Ca1/Si2, and Al/Si2 in Channel 1. The intensity of Al was

210 the sum of Al1 and Al2. For the intensity ratio of the same element from different upper energy levels $I_{i,j1}/I_{i,j2}$,

211 Mg1 (ion, 279.55nm, 280.27nm)/Mg2 (atom, 285.21nm) was defined as the plasma temperature indicator,

212 which showed the relation with the plasma temperature [16].

213

214 4.1 Pulse width effect on plasma temperature

215 Plasma temperature indicator I_{Mg1}/I_{Mg2} was evaluated in different delay time, which means the plasma

216 evolution process. The dependence of I_{Mg1}/I_{Mg2} on delay time using different lasers under different CO_2

217 concentration conditions is shown in Fig.4. From Fig.4, the plasma temperature was not affected by the CO_2

218 concentration obviously. However, the plasma temperature decreased when delay time increased. Comparing

219 Fig.4 (a) and Fig.4 (b), the plasma states using two nanosecond lasers had obvious differences. When delay

220 time was 300ns using Laser 1, I_{Mg1}/I_{Mg2} was averagely 7.65 under different CO_2 concentration conditions.

221 While using Laser 2, I_{Mg1}/I_{Mg2} was averagely only 3.03 when delay time was 5ns. The setting of delay time

222 with Laser 1 cannot be shorter than 300ns, because the plasma temperature would be very high and the

223 emission intensity would be very strong, saturating the ICCD detector. But it can be understood that the

224 plasma temperature would be much higher if in delay time of 5ns using Laser 1. Considering that the delay

225 time of 5ns was just after the plasma formation, it means at the formation time, plasma temperature using

226 Laser 1 was much higher than that using Laser 2. Along the evolution of plasma, using Laser 1, I_{Mg1}/I_{Mg2}

227 varied as 7.65, 5.66, 4.51, 3.50, 2.00 from 300ns to 1500ns, with obvious dependence on delay time. While

228 using Laser 2, I_{Mg1}/I_{Mg2} varied as 3.03, 3.02, 2.96, 2.75, 2.44 when delay time increased from 5ns to 100ns,

229 with less dependence on delay time.

230 The high plasma temperature can introduce some problems for the LIBS measurement. The measured

231 spectra without CO_2 in delay time of 300ns using Laser 1 are shown in Fig.5. Comparing Fig.5 in delay time

232 of 300ns and Fig.3 (a) in delay time of 800ns, the background signal was not horizontal and some emission

233 lines were immersed in the background signals at higher plasma temperature in Fig.5. The Al line

234 background in Fig.3 (a) was 0.048, and in Fig.5 was 0.185. At high plasma temperature, some effects

235 influence the background, such as the strong bremsstrahlung, wide line broadenings, or self-absorption.

236 What's more, when the plasma temperature is high, the absolute emission intensity is strong, which is easy

237 to saturate for the detector. The spectra behaviors change with the plasma formation and emission processes

238 [36]. The measured spectra using Laser 2 in delay time of 10ns and 100ns are shown in Fig.6, the

239 backgrounds of Al line were 0.037 and 0.033, which didn't show the obvious variation of the spectra in

240 different delay time, so the signal background could be clearly judged.

241 According to the theory, when using short 1ns pulse width laser, more energy is allocated to solid

242 breakdown. While using long 6ns pulse width laser, plasma can be more reheated during gas breakdown.

243 From Fig.4, it has testified that the plasma formation processes have obvious differences when using 6ns

244 pulse width laser and 1ns pulse width laser, and plasma reheating processes have more obvious influence to

245 increase plasma temperature. When using 1ns, the plasma temperature at the formation time was lower and

246 had less dependence on delay time.

247 The obvious dependence on delay time of spectra will induce the variation of the signal in the practical

248 measurement. Because plasma formation process is very fast and not fixed, obvious dependence on delay

249 time means plasma states have obvious differences with different delay time. In this way, the setting of delay

250 time should carefully consider plasma evolution process. However, for Laser 2, the setting of delay time will

251 be more robust. When the LIBS spectra are stabilized, it is benefit for the LIBS measurement of the powder

252 flow.

253

254 4.2 Pulse width effect on C signal

255 4.2.1 Surrounding CO_2 effects using different pulse width lasers

256 The laser pulse width not only affects the plasma states, but also the breakdown of surrounding gas. The

257 surrounding gas can also be broken down to generate the plasma. For example, the breakdown of

258 surrounding CO_2 in fly ash emits the carbon signal, which results in the spurious carbon signal to increase

259 the calculated unburned carbon content in fly ash.

260 The comparison of the spectra using two different lasers should be at similar plasma states. When delay

261 time was 1000ns using Laser 1, I_{Mg1}/I_{Mg2} showed the similar level as that using Laser 2. As for Laser 2, when

262 delay time was 5ns and 10ns, even though I_{Mg1}/I_{Mg2} showed the similar level as Laser 1, there would be

263 other effects influencing signals just after plasma formation, so they were not suitable for the comparison.

264 While after delay time of 50ns, I_{Mg1}/I_{Mg2} was relatively small. Therefore, the measured spectra in delay time

265 of 25ns using Laser 2 were compared with that in delay time of 1000ns using Laser 1 because of their

266 similar plasma temperature.

267   The measured spectra of fly ash without CO_2 and with 3.80% CO_2 are shown in Fig.7 using Laser 1 in

268 delay time of 1000ns in Channel 2. Comparing Fig.7 (a) and Fig.7 (b), when CO_2 concentration increased

269 from 0% to 3.80%, the C emission line intensity increased from 0.298 to 0.439. The C signal from the CO_2

270 breakdown resulted in the inaccurately quantitative analysis of the unburned carbon content in fly ash. The

271 measured spectra of fly ash with different CO_2 concentration using Laser 2 in delay time of 25ns in Channel

272 2 are shown in Fig.8. Comparing Fig.8 (a) without CO_2 and Fig.8 (b) with 3.80% CO_2, the C emission line

273 intensity changed from 0.257 to 0.259, which didn't show the obvious change compared to that using Laser

274 1.

275   Therefore, the breakdown rate of surrounding gas was different from different lasers due to the pulse

276 width effect. When the laser pulse width was shorter, such as 1ns, the breakdown rate of the surrounding gas

277 decreased. The C signal from the CO_2 breakdown reduced.

278   According to the measured spectra, the dependence of I_C/I_{Si1} on CO_2 concentration is shown in Fig.9.

279 Compared with I_C/I_{Si1} under 0% CO_2 condition, when the CO_2 concentration increased, the maximum

280 enhancement of I_C/I_{Si1} using Laser 1 was 41.2%, while the maximum enhancement of I_C/I_{Si1} using Laser 2

281 was 26.7%. The intensity enhancement of I_C/I_{Si1} using Laser 1 was higher than that using Laser 2. It

282 indicated that the CO_2 effect on unburned carbon measurement of solid fly ash powder could be reduced

283 when using Laser 2. The increase of I_C/I_{Si1} with CO_2 in Fig.9 didn't follow the linear relation due to the non-

284 uniformity of the fly ash powder and the mixture of powder and surrounding gas [19]. The measured carbon

285 signals contained both the powder carbon signal and gas carbon signal. The fluctuation of the powder flow

286 caused the fluctuation and inhomogeneity of the plasma. Therefore, one of the merits of fly ash

287 measurement using Laser 2 is the reduction of gas breakdown to diminish the CO_2 effect on unburned

288 carbon measurement because of the effect on the solid powder and gas plasma processes, which can be

289 applicable for other powder conditions. Another merit is that Laser 2 is a microchip laser with high

290 durability and long lifetime. Laser 2 employed here is more available for online measurement of LIBS

291 system due to its flexibility and durability.

292

293   4.2.2 Plasma temperature correction of C signal

294   According to the previous study, the carbon signal intensity was affected by the plasma temperature [3,

295   16]. As shown in Fig.4, plasma temperature showed the obvious delay time dependence using Laser 1.

296   However, the plasma temperature showed a little change using Laser 2. Plasma temperature correction is

297   necessary to reduce the plasma temperature effect on signals, especially for the measurement using Laser 1.

298   The temperature correction factor for carbon signal was determined according to the relation between I_C/I_{Si1}

299   and I_{Mg1}/I_{Mg2}. The variation of plasma temperature with delay time was different using different lasers.

300   Therefore, the plasma temperature correction factor for each laser was determined respectively including all

301   the CO_2 concentration and delay time conditions.

302   After applying the plasma temperature correction, the relation between the corrected I_C/I_{Si1} and CO_2

303   concentration is shown in Fig.10. In Fig.10, the corrected I_C/I_{Si1} in each CO_2 concentration condition was the

304   averaged result in all delay time. After plasma temperature correction, the maximum enhancement of I_C/I_{Si1}

305   using Laser 1 was 30.4%, and the maximum enhancement of I_C/I_{Si1} using Laser 2 was 19.7%. Compared

306   with Fig.9, the enhancement of I_C/I_{Si1} decreased after the plasma temperature correction. As for the standard

307   deviation, the largest standard deviation in Fig.9 was 0.0712 of Laser 1 and 0.0646 of Laser 2, while the

308   largest standard deviation in Fig.10 was 0.0649 of Laser 1 and 0.0624 of Laser 2. Plasma temperature

309   correction didn't make obvious difference on standard deviation. In a word, plasma temperature correction

310   can partially decrease the influence of surrounding CO_2 breakdown.

311

312   4.3 Pulse width effect on solid breakdown signals

313   According to the C quantitative calculation equation, solid powder breakdown signals of I_{Ca1}/I_{Si2}, I_{Fe}/I_{Si2},

314   I_{Al}/I_{Si2} should also be concerned [16]. So the pulse width effect on these solid powder breakdown signals

315   was also discussed here. As mentioned in Theory, for 6ns pulse width laser, more energy is introduced to

316   plasma reheating process, while for 1ns pulse width laser, more energy is allocated to solid breakdown. In

317   order to study the pulse width effect on these solid powder breakdown signals, I_{Ca1}/I_{Si2} was discussed here in

318   detail under different experimental conditions. I_{Fe}/I_{Si2}, I_{Al}/I_{Si2} showed the consistent results [3, 16]. In the

319 case of I_C/I_{Si1} analysis which was affected by the surrounding CO_2 gas, it has been discussed above in detail.

320 The CO_2 concentration dependencies of I_{Ca1}/I_{Si2} in different delay time when using Laser 1 and Laser 2

321 are shown in Fig.11. I_{Ca1}/I_{Si2} didn't show the obvious change with CO_2 concentration. When using Laser 1,

322 the averaged I_{Ca1}/I_{Si2} under different CO_2 concentration conditions was as high as 0.575 in delay time of

323 300ns, and it decreased as delay time increased, varying as 0.536, 0.496, 0.380, 0.225, due to the higher

324 upper energy level of Ca1 than that of Si2. However, the averaged I_{Ca1}/I_{Si2} using Laser 2 had less variation,

325 varying as 0.342, 0.349, 0.347, 0.308, and 0.297 along the increase of delay time. Using Laser 2, I_{Ca1}/I_{Si2}

326 also had less dependence on delay time compared with that using Laser 1. The values of I_{Ca1}/I_{Si2} using Laser

327 2 in different delay time were similar as that using Laser 1 in delay time of 1000ns. The results in Fig.11

328 corresponded to the plasma temperature in Fig.4. Therefore, it indicated that plasma temperature has crucial

329 effects on the solid breakdown signals. The signal stability under different lasers was also different, and the

330 large relative standard deviation indicated the fluctuation of signals. For Laser 1, 8 results of total 20 results

331 in Fig.11 (a) had the relative standard deviation more than 10%, and 3 of them were more than 20%. For

332 Laser 2, 6 results in Fig.11 (b) had the relative standard deviation more than 10%, while only 1 of them was

333 more than 20%. So the signals using Laser 2 had less fluctuations, which is beneficial for the measurement.

334

335 **5. Conclusions**

336

337 The unburned carbon in fly ash is an important factor to evaluate combustion efficiency. The low carbon

338 content in fly ash means the good combustion of the boiler. Besides, the recycling of the fly ash also requires

339 the low carbon content in fly ash. Online measurement of fly ash compositions helps to control the carbon

340 content of fly ash, and LIBS technology can realize the online measurement compared to other methods. The

341 LIBS measurement of fly ash powder flow should consider both the solid powder breakdown and

342 surrounding gas breakdown, while the surrounding gas breakdown will introduce the carbon signal from

343 CO_2 gas to the unburned carbon measurement of fly ash. Experiments were designed using 6ns pulse width

344 laser and 1ns pulse width laser to measure fly ash seperately to compare their properties. The results are

345 concluded as follow.

346   1. At the formation time of plasma, plasma temperature using 6ns pulse width laser was much higher than

347   that using 1ns pulse width laser. High plasma temperature affected the background of spectra and

348   measurement accuracy. Using 6ns pulse width laser, the plasma temperature had obvious dependence on

349   delay time, the parameters setting should consider the plasma states. It has testified that when the laser pulse

350   width changes from 6ns to 1ns, the plasma formation process had obvious change, which showed the lower

351   plasma temperature at the formation time, more stable background, and less dependence on delay time.

352   2. The I_C/I_{Si1} increased obviously with the increase of the CO_2 concentration when using 6ns pulse width

353   laser. The CO_2 concentration dependence of I_C/I_{Si1} was reduced when using 1ns pulse width laser under all

354   the CO_2 concentration conditions. The CO_2 effect on unburned carbon measurement could be reduced when

355   using 1ns pulse width laser. When applying the plasma temperature correction method, the increase of I_C/I_{Si1}

356   with the CO_2 concentration became smaller.

357   3. The laser pulse width also influenced the solid breakdown signals stability. The powder breakdown

358   signals using 1ns pulse width laser showed less delay time dependence and generally smaller relative

359   standard deviations than that using 6ns pulse width laser.

360   In summary, the CO_2 effect on the unburned carbon signal can be reduced when using the laser with pulse

361   width of 1ns, which also induces less variation of plasma temperature and solid powder breakdown signals

362   like I_{Ca1}/I_{Si2}, I_{Fe}/I_{Si2}, I_{Al}/I_{Si2}. All these are beneficial for fly ash flow measurement. At the same time, the laser

363   with pulse width of 1ns is a microchip laser with high durability and long lifetime, which is more suitable

364   for the LIBS system integration for the industrial online application. In a word, 1ns pulse width laser is more

365   suitable for the fly ash powder flow measurement using LIBS.

366

367   **Acknowledgements**

368

371

372   **References**

[1]. Kazemian H, Naghdali Z, Kashani T G, et al, Conversion of high silicon fly ash to Na-P1 zeolite: Alkaline fusion followed by hydrothermal crystallization, Advanced Powder Technology, 21 (2009) 279-283.

[2]. Noda N, Makino H, Influence of operating temperature on performance of electrostatic precipitator for pulverized coal combustion boiler, Advanced Powder Technology, 21 (2010) 495-499.

[3]. Noda M, Deguchi Y, Iwasaki S, et al, Detection of carbon content in a high-temperature and high-pressure environment using laser-induced breakdown spectroscopy, Spectrochimica Acta Part B Atomic Spectroscopy, 57 (2002) 701-709.

[4]. A.K. Ouazzane, J.L. Castagner, A.R. Jones, et al, Design of an optical instrument to measure the carbon content of fly ash, Fuel, 81 (2002) 1907-1911.

[5]. Y. Qiu, M.C. Tian, L. Cheng, et al, The Theory of the Reduction of Fly-ash Carbon Content in a Circulating Fluidized Boiler and Its Applied Research, 20 (2005) 369-373.

[6]. Xie H L, Zhang, The Necessity of Monitoring Carbon Content in Fly-ash and the Development of Measuring Technique, Science Technology & Engineering, 16 (2016) 115-121.

[7]. Cheng Q M, Xiao-Qing H U, Wang Y F, et al, Summary of Measurement Methods of Carbon Content in Fly Ash, Journal of Shanghai University of Electric Power, 27 (2011) 519-524.

[8]. Marrero J, Polla G, Rebagliati R J, et al, Characterization and determination of 28 elements in fly ashes collected in a thermal power plant in Argentina using different instrumental techniques, Spectrochimica Acta Part B Atomic Spectroscopy, 62 (2007) 101-108.

[9]. Tanaka H, Fujii A, Fujimoto S, et al, Microwave-Assisted Two-Step Process for the Synthesis of a Single-Phase Na-A Zeolite from Coal Fly Ash, Advanced Powder Technology, 19 (2008) 83-94.

[10]. Li Q, Pang J, Wang B, et al, Preparation, characterization and microwave absorption properties of barium-ferrite-coated fly-ash cenospheres, Advanced Powder Technology, 24 (2013) 288-294.

[11]. Chindaprasirt P, Role of microwave radiation in curing the fly ash geopolymer, Advanced Powder Technology, 24 (2013) 703-707.

[12]. Y. Deguchi, Industrial applications of laser diagnostics, CRC Press, 2011.

399 [13]. Wang Z Z, Deguchi Y, Zhang Z Z, et al, Laser-induced breakdown spectroscopy in Asia, Frontiers of

400 Physics, 11 (2016) 231-255.

401 [14]. Wang Z, Yuan T B, Hou Z Y, et al, Laser-induced breakdown spectroscopy in China. Frontiers of

402 Physics, 9 (2014) 419-438.

403 [15]. Zhang L, Ma W G, Yan X J, et al, Research on parameters optimization of laser-induced breakdown

404 spectroscopy based experimental device, Spectroscopy & Spectral Analysis, 31 (2011) 2355-2360.

405 [16]. Wang Z Z, Deguchi Y, Kuwahara M, et al, Quantitative elemental detection of size-segregated

406 particles using laser-induced breakdown spectroscopy, Spectrochimica Acta Part B Atomic Spectroscopy,

407 87 (2013) 130-138.

408 [17]. Bai K J, Tian H C, Yao S C, et al, Influence of laser energy on measurement of unburned carbon in fly

409 Ash particle flow, Spectroscopy & Spectral Analysis, 34 (2014) 1407.

410 [18]. S. C. Yao, J. D. Lu, C. L. Xie, et al, Quantitative analysis of laser induced carbon plasma by intensity

411 ratio calibration, High Power Laser and Particle Beams, 20 (2008) 1089-1092.

412 [19]. Wang Z Z, Deguchi Y, Watanabe H, et al, Improvement on Quantitative Measurement of Fly Ash

413 Contents Using Laser-Induced Breakdown Spectroscopy, Journal of Flow Control Measurement &

414 Visualization, 03 (2015) 10-21.

415 [20]. Yao S, Lu J, Zheng J, et al, Analyzing unburned carbon in fly ash using laser-induced breakdown

416 spectroscopy with multivariate calibration method, Journal of Analytical Atomic Spectrometry, 27 (2012)

417 473-478.

418 [21]. Zhang T, Yan C, Qi J, et al, Classification and discrimination of coal ash by laser-induced breakdown

419 spectroscopy (LIBS) coupled with advanced chemometric methods, Journal of Analytical Atomic

420 Spectrometry, 32 (2017) 1960-1965.

421 [22]. Stankova A, Gilon N, Dutruch L, et al, A simple LIBS method for fast quantitative analysis of fly

422 ashes, Fuel, 89 (2010) 3468-3474.

423 [23]. Ctvrtnickova T, Mateo M P, Yañez A, et al, Characterization of coal fly ash components by laser-

424 induced breakdown spectroscopy, Spectrochimica Acta Part B Atomic Spectroscopy, 64 (2009) 1093-1097.

[24]. Zhao Q X, Zhang Z X, Wen-Zhi D U, et al, Experimental Study on Sulfuric Acid Dewpoint Corrosion in Simulated Atmospheric Conditions, Journal of Chinese Society of Power Engineering, 32 (2012) 420-424.

[25]. J. T. Bian, K. J. Yin, S. C. Yao, et al, Quantitative Analysis of Unburned Carbon in Fly Ash by Laser-Induced Breakdown Spectroscopy in Different Atmosphere, Laser & Optoelectronics Process, 4 (2016) 234-239.

[26]. Kurihara M, Ikeda K, Izawa Y, et al, Optimal boiler control through real-time monitoring of unburned carbon in fly ash by laser-induced breakdown spectroscopy, Appl Opt, 42 (2003) 6159-6165.

[27]. Zhang L, Jia S T, Hu Z Y, et al, Recent progress on laser-induced breakdown spectroscopy for the monitoring of coal quality and unburned carbon in fly ash, Frontiers of Physics, 7 (2012) 690-700.

[28]. Zhang L, Ma W, Dong L, et al, Development of an apparatus for online analysis of unburned carbon in fly ash using laser-induced breakdown spectroscopy (LIBS), Applied Spectroscopy, 65 (2011) 790-796.

[29]. Wang Z Z, Deguchi Y, Kuwahara M, et al, Enhancement of Laser-Induced Breakdown Spectroscopy (LIBS) Detection Limit Using a Low-Pressure and Short-Pulse Laser-Induced Plasma Process, Applied Spectroscopy, 67 (2013) 1242-1251.

[30]. Eland K L, Stratis D N, Lai T, et al, Some Comparisons of LIBS Measurements using Nanosecond and Picosecond Laser Pulses, Applied Spectroscopy, 55 (2001) 279-285.

[31]. Rieger G W, Taschuk M, Tsui Y Y, et al, Comparative study of laser-induced plasma emission from microjoule picosecond and nanosecond KrF-laser pulses, Spectrochimica Acta Part B Atomic Spectroscopy, 58 (2003) 497-510.

[32]. Rohwetter P, Yu J, Méjean G, et al. Remote LIBS with ultrashort pulses: characteristics in picosecond and femtosecond regimes[J]. Journal of Analytical Atomic Spectrometry, 19 (2004) 437-444.

[33]. Abdel-Salam Z A, Nanjing Z, Anglos D, et al, Effect of experimental conditions on surface hardness measurements of calcified tissues via LIBS, Applied Physics B, 94 (2009) 141-147.

[34]. S. V. Rao, S. Sreedhar, M. A. Kumar, P. P. Kiran, S. P. Tewari and G. M. Kumar, Laser Induced Breakdown Spectroscopy of high energy materials using nanosecond, picosecond, and femtosecond pulses: Challenges and opportunities, Proc. SPIE, 2011, 8173.

451   [35]. Labutin T A, Lednev V N, Ilyin A A, et al, Femtosecond Laser-Induced Breakdown Spectroscopy,

452   Journal of Analytical Atomic Spectrometry, 31 (2015) 90-118.

453   [36]. Noll R. Laser-induced breakdown spectroscopy: fundamentals and applications, Springer, 2011.

454   [37]. Bye C A, Scheeline A., Saha-Boltzmann Statistics for Determination of Electron Temperature and

455   Density in Spark Discharges Using an Echelle/CCD System, Applied Spectroscopy, 47 (1993) 2022-2030.

456   [38]. Naeem T M, Matsuta H, Wagatsuma K, Effect of plasma gas for spectrometric analysis of tin and zinc

457   using low-pressure laser-induced plasma, Spectrochimica Acta. Part B: Atomic Spectroscopy, 58 (2003)

458   891-899.

459   [39]. Cristoforetti G, Legnaioli S, Palleschi V, et al, Characterization of a collinear double pulse laser-

460   induced plasma at several ambient gas pressures by spectrally- and time-resolved imaging, Applied Physics

461   B: Lasers and Optics, 80 (2005) 559-568.

462   [40]. Yao S C, Chen J C, Lu J D, et al, Influence of C-Fe Lines Interference Correction on Laser-Induced

463   Breakdown Spectroscopy Measurement of Unburned Carbon in Fly Ash, Spectroscopy & Spectral Analysis,

464   35 (2015) 1719-1723.

465   [41]. Bai K, Yao S, Lu J, et al, Correction of C-Fe line interference for the measurement of unburned carbon

466   in fly ash by LIBS[J]. Journal of Analytical Atomic Spectrometry, 31 (2016) 3418-2426.

467   [42]. Y. Ralchenko, NIST atomic spectra database. Laboratory Space Science Workshop, 1998.

468   https://physics.nist.gov/PhysRefData/ASD/lines_form.html

469

470

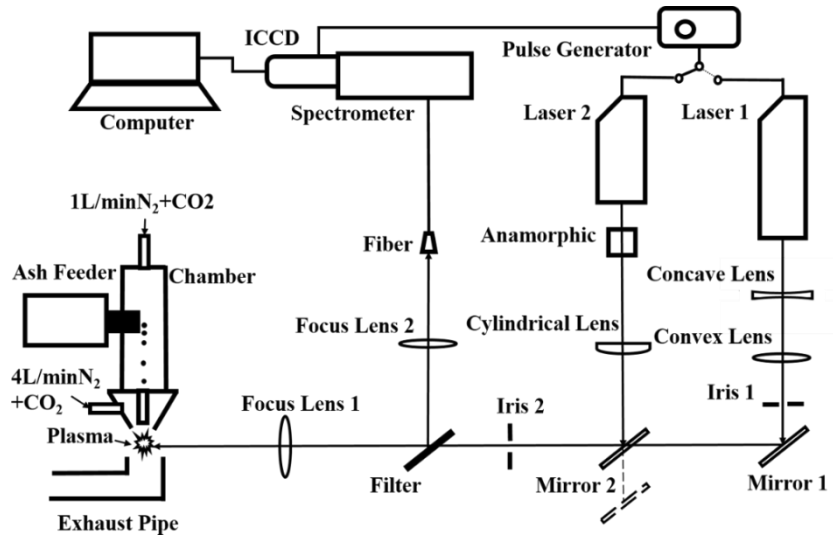**Figure Captions**

Fig.1 Plasma development processes during LIBS.

Fig.2 Fly ash measurement system of LIBS using different lasers.

Fig.3 Measured spectra of fly ash without CO_2 using Laser 1. Conditions: pulse width: 6ns, delay time: 800ns.

Fig.4 Delay time dependence of I_{Mg1}/I_{Mg2} using different lasers under different CO_2 concentration conditions.

Fig.5 Measured spectra without CO_2 using Laser 1 in Channel 1. Conditions: pulse width: 6ns, delay time: 300ns, resolution of 0.076nm/pixel.

Fig.6 Measured spectra without CO_2 using Laser 2 in Channel 1 in different delay time. Conditions: pulse width: 1ns, resolution of 0.076nm/pixel.

Fig.7 Comparison of measured spectra of fly ash with different CO_2 concentration using Laser 1 in Channel 2. Conditions: pulse width: 6ns, delay time: 1000ns, resolution: 0.012nm/pixel.

Fig.8 Comparison of measured spectra of fly ash with different CO_2 concentration using Laser 2 in Channel 2. Conditions: pulse width: 1ns, delay time: 25ns, resolution: 0.012nm/pixel.

Fig.9 Dependence of I_C/I_{Si1} on CO_2 concentration using different lasers in Channel 2. Conditions of Laser 1: pulse width: 6ns, delay time: 1000ns. Conditions of Laser 2: pulse width: 1ns, delay time: 25ns.

Fig.10 Dependence of averaged I_C/I_{Si1} on CO_2 concentration after plasma temperature correction in Channel 2. Conditions: pulse width of Laser 1: 6ns, pulse width of Laser 2: 1ns.

Fig.11 Dependence of I_{Ca1}/I_{Si2} on CO_2 concentration in different delay time using Laser 1 and Laser 2. Conditions: Laser 1, pulse width: 6ns, delay time: 300ns, 500ns, 800ns, 1000ns, 1500ns. Laser 2, pulse width: 1ns, delay time: 5ns, 10ns, 25ns, 50ns, 100ns.

Fig.1
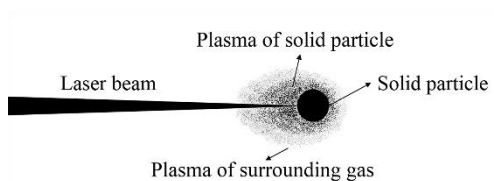
(a) Plasma structure concept of powder with surrounding gas
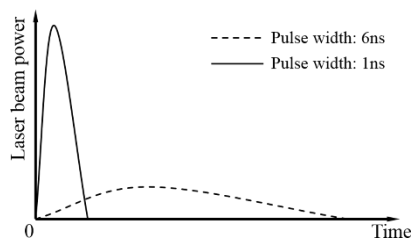
(b) Diagram of the laser pulse width
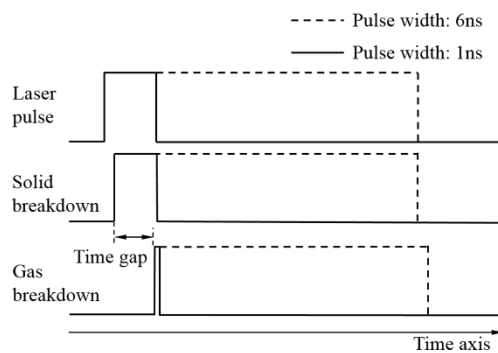
(c) Concept of time evolution process during laser-induced plasma

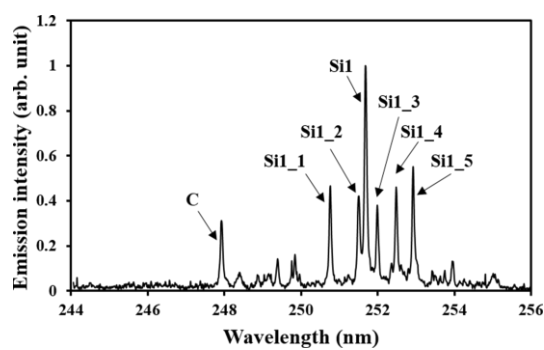Fig.1 Plasma development processes during LIBS.

Fig.2

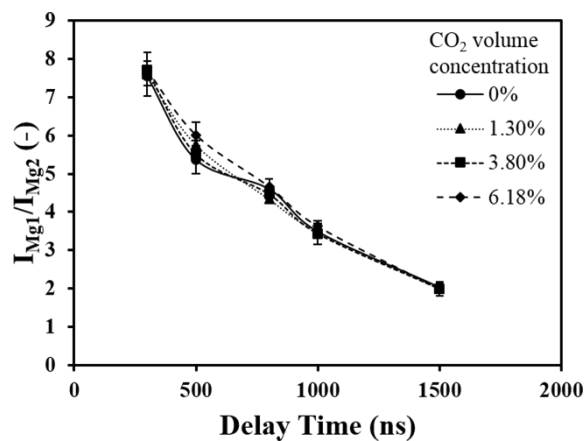Fig.2 Fly ash measurement system of LIBS using different lasers.
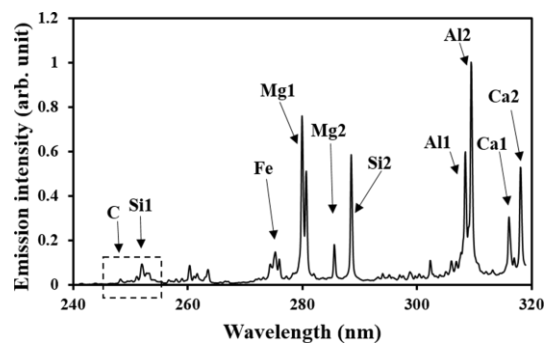
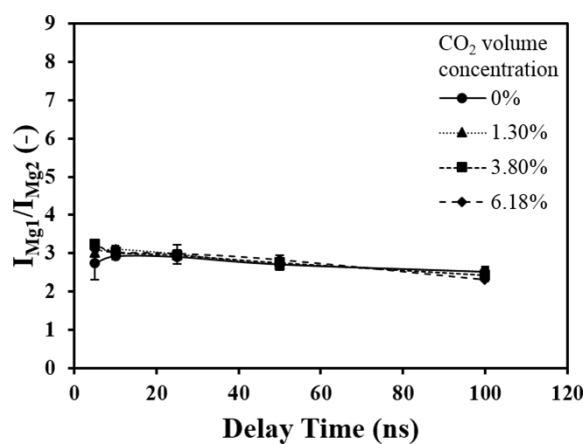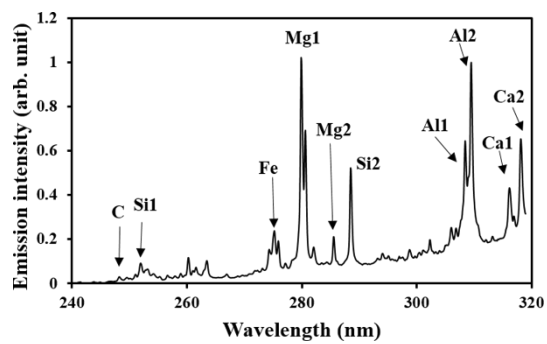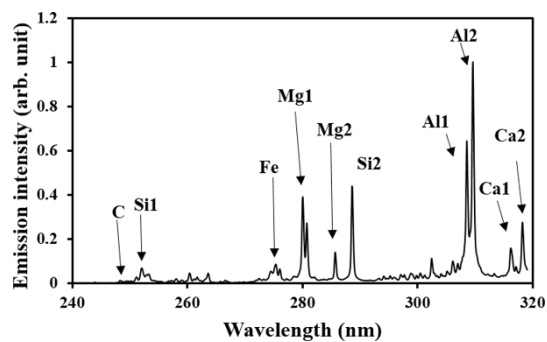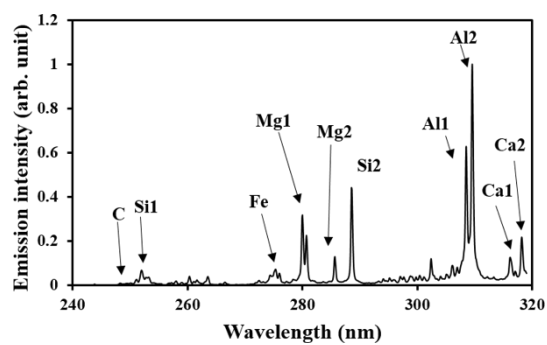**Fig.3**

(a) Channel 1 with resolution of 0.076nm/pixel

(b) Channel 2 with resolution of 0.012nm/pixel

Fig.3 Measured spectra of fly ash without CO_2 using Laser 1. Conditions: pulse width: 6ns, delay time: 800ns.

Fig.4

(a) Laser 1 with pulse width of 6ns

(b) Laser 2 with pulse width of 1ns

Fig.4 Delay time dependence of I_{Mg1}/I_{Mg2} using different lasers under different CO_2 concentration

conditions.

Fig.5

Fig.5 Measured spectra without CO_2 using Laser 1 in Channel 1. Conditions: pulse width: 6ns, delay time:

300ns, resolution of 0.076nm/pixel.

Fig.6

(a) Delay time of 10ns

(b) Delay time of 100ns

Fig.6 Measured spectra without CO_2 using Laser 2 in Channel 1 in different delay time. Conditions: pulse

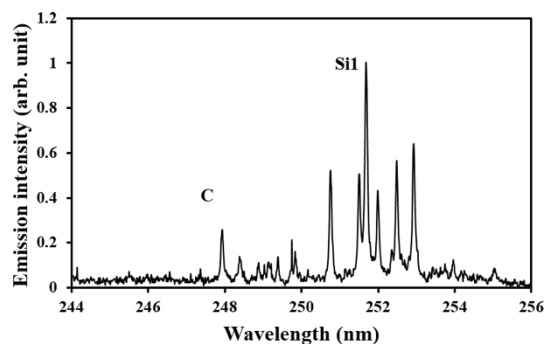width: 1ns, resolution of 0.076nm/pixel.
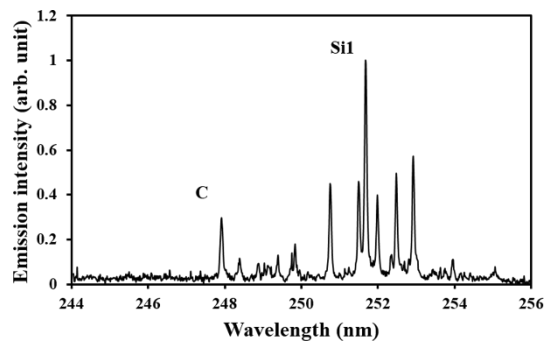
Fig.7

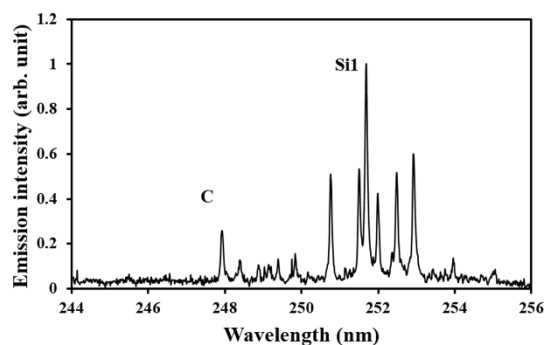

(a) Without CO_2
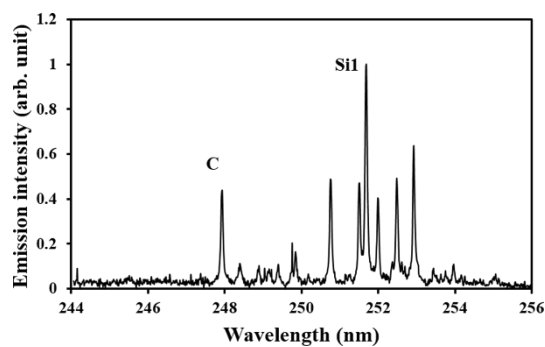
(b) With 3.80% CO_2

Fig.7 Comparison of measured spectra of fly ash with different CO_2 concentration using Laser 1 in Channel 2. Conditions: pulse width: 6ns, delay time: 1000ns, resolution: 0.012nm/pixel.

Fig.8

(a) Without CO_2

(b) With 3.80% CO_2

Fig.8 Comparison of measured spectra of fly ash with different CO_2 concentration using Laser 2 in

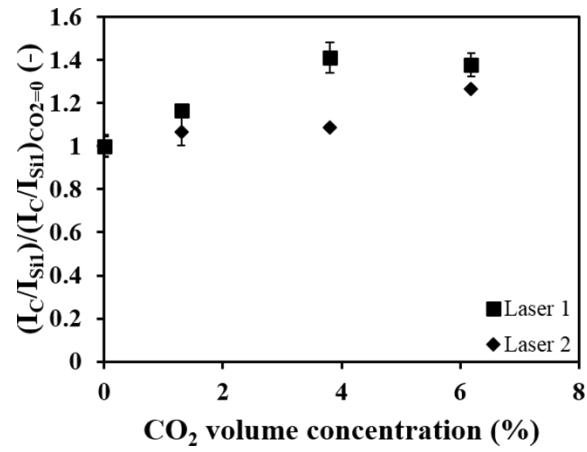Channel 2. Conditions: pulse width: 1ns, delay time: 25ns, resolution: 0.012nm/pixel.

Fig.9

Fig.9 Dependence of I_C/I_{Si1} on CO_2 concentration using different lasers in Channel 2. Conditions of Laser 1:

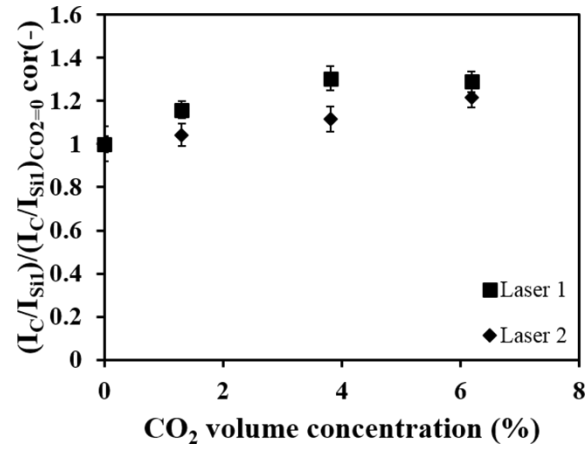pulse width: 6ns, delay time: 1000ns. Conditions of Laser 2: pulse width: 1ns, delay time: 25ns.

Fig.10

Fig.10 Dependence of averaged I_C/I_{Si1} on CO_2 concentration after plasma temperature correction in

Channel 2. Conditions: pulse width of Laser 1: 6ns, pulse width of Laser 2: 1ns.
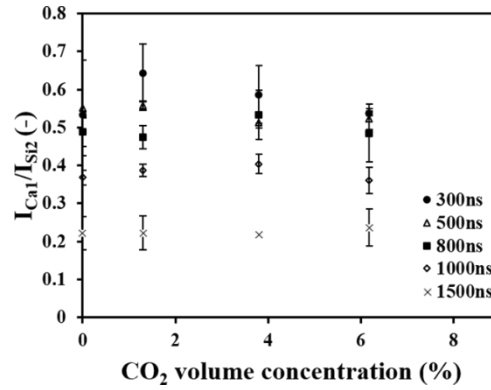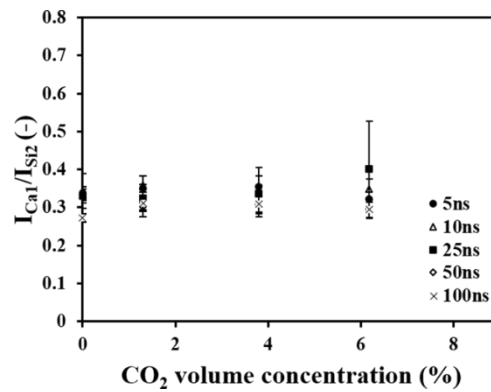
Fig.11

(a) I_{Ca1}/I_{Si2} using Laser 1

(b) I_{Ca1}/I_{Si2} using Laser 2

Fig.11 Dependence of I_{Ca1}/I_{Si2} on CO_2 concentration in different delay time using Laser 1 and Laser 2.

Conditions: Laser 1, pulse width: 6ns, delay time: 300ns, 500ns, 800ns, 1000ns, 1500ns. Laser 2, pulse

width: 1ns, delay time: 5ns, 10ns, 25ns, 50ns, 100ns.

Tables

Table 1 Main compositions of fly ash sample

Table 2 Measured species and the specific wavelengths [42]

Table 1

Table 1 Main compositions of fly ash sample

Ash Content (wt%)										Unburned Carbon (wt%)
SiO_2	Al_2O_3	Fe_2O_3	K_2O	CaO	TiO_2	P_2O_5	SO_3	MgO	Na_2O	
37.38	25.91	6.26	0.39	1.36	0.8	0.36	0.53	0.59	0.78	24.9

Table 2

Table 2 Measured species and the specific wavelengths [42]

species	wavelength(nm)	E_i(cm^{-1})	E_k(cm^{-1})
C	247.86	21648.01	61981.82
Si1	251.61	223.16	39955.053
Si1_1	250.69	77.12	39955.053
Si1_2	251.43	0	39760.29
Si1_3	251.92	77.12	39760.29
Si1_4	252.41	77.12	39683.16
Si1_5	252.85	223.16	39760.29
Si2	288.16	6298.85	40991.884
Fe	274.20-	415.93-	36686.16-
(atom and ion)	275.63	8846.7	45289.80
Ca1(ion)	315.89	25191.51	56839.25
Ca2 (ion)	318.13	25414.4	56839.25
Al1	308.22	0	32435.45
Al2	309.27	112.06	32436.79
Mg1 (ion)	279.55	0	35760.88
Mg1 (ion)	280.27	0	35669.31
Mg2	285.21	0	35051.26